scientific reports

OPEN

Discovery of miRNA–mRNA regulatory networks in glioblastoma reveals novel insights into tumor microenvironment remodeling

Iulia A. Grigore[1,3], Athulram Rajagopal[1,3], Jonathan Tak-Sum Chow[1], Thomas J. Stone[2] & Leonardo Salmena[1✉]

Adult glioblastoma (GBM) is a highly aggressive primary brain tumor, accounting for nearly half of all malignant brain tumors, with a median survival rate of only 8 months. Treatment for GBM is largely ineffective due to the highly invasive nature and complex tumor composition of this malignancy. MicroRNAs (miRNA) are short, non-coding RNAs that regulate gene expression by binding to messenger RNAs (mRNA). While specific miRNA have been associated with GBM, their precise roles in tumor development and progression remain unclear. In this study, the analysis of miRNA expression data from 743 adult GBM cases and 59 normal brain samples identified 94 downregulated miRNA and 115 upregulated miRNA. Many of these miRNA were previously linked to GBM pathology, confirming the robustness of our approach, while we also identified novel miRNA that may act as potential regulators in GBM. By integrating miRNA predictions with gene expression data, we were able to associate downregulated miRNA with tumor microenvironment factors, including extracellular matrix remodeling and signaling pathways involved in tumor initiation, while upregulated miRNA were found to be associated with essential neuronal processes. This analysis highlights the significance of miRNA in GBM and serves as a foundation for further investigation.

Keywords microRNA, Glioblastoma, Tumor microenvironment, Extracellular matrix, Growth signaling

Glioblastoma multiforme (GBM) is classified as a grade IV *IDH*-wildtype diffuse glioma[1]. GBM is the most aggressive malignant primary brain tumor which accounts for nearly half of all malignant brain tumors, and affects approximately 7 out of every 100,000 older adults every year[2]. The majority of GBM patients succumb to the malignancy with a median survival time of approximately 8 months from diagnosis[2]. A common hallmark of GBM is its rapid infiltration and growth into the surrounding brain parenchyma, posing significant challenges for surgical resection[3]. Furthermore, the presence of GBM stem cells complicates treatment efficacy due to their chemo- and radioresistance[4,5]. In sum, there is a critical need to gain a deeper understanding of GBM biology before effective treatment strategies can be realized.

GBM is a malignancy characterized by a complex tumor microenvironment (TME) that encompasses intricate interactions between transformed neuronal cells at different stages of differentiation[6,7] as well as non-cancerous cells including neurons and fibroblasts, which significantly contribute to tumor growth and progression[8–10]. The GBM microenvironment also features a diverse range of immune cells, such as macrophages and T regulatory lymphocytes which possess suppressive qualities that can create a "cold" tumor environment[9,11,12]. In sum, through direct interactions or crosstalk with resident cells, GBM cells hijack the TME and surrounding extracellular matrix (ECM) to enhance tumor malignancy[9,13,14].

MicroRNAs (miRNA) are short non-coding RNA molecules essential for post-transcriptional gene regulation, capable of silencing the expression of various genes, both protein-coding and non-coding[15–17]. Through partial Watson–Crick complementarity, miRNA hybridize with RNA molecules and exert their regulatory functions

[1]Department of Pharmacology and Toxicology, University of Toronto, Toronto, ON, Canada. [2]Developmental Biology and Cancer Research and Teaching Department, UCL GOS Institute of Child Health, University College London, London, UK. [3]These authors contributed equally: Iulia A. Grigore and Athulram Rajagopal. ✉email: leonardo.salmena@utoronto.ca

by inducing RNA cleavage or translational repression[16,18]. Emerging studies suggest that dysregulated miRNA expression plays a role in promoting tumor hallmarks in GBM[19], and can serve as prognostic markers for patient survival[20]. Furthermore, preclinical studies have highlighted the potential of miRNA modulation as a treatment strategy for GBM[21,22].

While many miRNA associated with GBM progression have been reported, most remain unexplored. Understanding their new roles may reveal new insights into GBM biology and novel therapeutic strategies. However, the current knowledge gap stems in part from outdated and low-quality miRNA expression data from GBM patient miRNA microarray studies. Although next-generation technologies, including miRNA-seq and Nanostring data, are becoming more available, these datasets still face limitations, such as small sample sizes, low sensitivity, incomplete miRNA detection, uneven sample distribution, and insufficient matched controls[23-31]. In the absence of more optimal datasets, integrating available data increases the sample size and improves the statistical power and robustness of analyses. Indeed, two previous studies investigated the role of specific miRNA hits identified through the integration of multiple adult and pediatric GBM profiling datasets[32,33]. Extending previous research, we integrated additional datasets to create the largest-to-date collection of miRNA expression data from adult primary GBM patients. This study, therefore, provides the most comprehensive analysis of miRNA in GBM to date, with potential for further investigation as more data become available.

Our integrated analysis of miRNA prediction algorithms and protein-coding gene expression revealed links between downregulated miRNA and ECM factors and key growth and immune signaling pathways, and between upregulated miRNA and neuronal processes, suggesting a role in neuronal differentiation during GBM development. The potential for miRNA to promote GBM aggressiveness by remodeling the TME is particularly promising for therapeutic exploration. Our analyses identified both oncogenic and tumor-suppressive miRNA with novel functions in the molecular mechanisms driving GBM progression. These findings, together with the recent Nobel Prize in miRNA research, suggest novel hypotheses for miRNA regulation in GBM and may inspire innovative miRNA-targeted therapies[34].

Materials and methods
Data acquisition
Publicly available miRNA expression datasets were identified using the search terms, 'microRNA' and 'glioblastoma' on NCBI GEO and NCI databases between May 2023 and January 2024. All identified datasets were manually screened and filtered based on the following criteria: each dataset required a minimum of 3 brain tumor samples and 3 non-cancerous brain tissue controls. This study focuses on adult primary *IDH*-wildtype GBM. At the time of analysis, any samples identified as pediatric, recurrent, secondary or *IDH*-mutant were removed.

Data processing and quality control
Unprocessed miRNA expression data was accessed from the NCBI GEO and NCI platforms for GSE158284, GSE109628, GSE90603, GSE65626, GSE25631, GSE91014 (TCGA), GSE165937, GSE214252 and PDC000204 datasets. The following analyses were performed using the R programming language. Protocols can be shared upon request. For GSE158284, GSE109628 and GSE91014, miRNA expression data was imported using the AgiMicroRna package (2.48.0)[35]. For GSE90603 and GSE65626, CEL files were imported and read using the oligo package (1.60.0)[36]. For GSE25631, an illumina probe summary file was loaded using the limma package (3.54.2)[37]. Raw counts from GSE165937, GSE214252 and PDC000204 were downloaded and converted into an edgeR-compatible DGElist object (3.40.2)[38].

For microarray datasets, raw expression data underwent quantile normalization and background correction using microarray platform-specific packages including AgiMicroRna (2.48.0), oligo (1.60.0) and limma (3.54.2)[35,36,39,40]. Low-expression miRNA probes were removed from analyses if probes were not expressed or if expression values were below the mean expression of negative-control probes in a minimum of 50% of arrays within each individual dataset. For count-based datasets, raw counts were processed and normalized using the trimmed mean of M-samples method via the EdgeR package (3.40.2)[38]. Low expression miRNA were removed if they had a count value lower than 10 in a minimum of 70% of samples within each individual dataset. For consistency across datasets, miRNA nomenclature was converted to miRBase v22 using the miRBaseConverter package[41].

Each dataset was screened for sample outliers by assessing the miRNA expression distribution across samples using unsupervised principal component analysis (PCA). In the GSE158284 and GSE25631 datasets, potential outliers were detected by PCA clustering and additional platform-specific quality control tools were used. For GSE158284, the arrayQualityMetrics package was used to calculate the outlier detection threshold represented by the Kolmogorov–Smirnov statistic between the distribution of individual and combined data[42]. Five irregularly clustered samples exceeded the calculated outlier detection threshold of 0.233 (Supplementary Fig. S1). For GSE25631, the platform-specific detection *P*-values were used as a measure of sample quality. Sixteen samples that clustered distantly based on PCA showed to have a 15% increased proportion of failed probes (*P*-value < 0.0001) (Supplementary Fig. S1). These five (GSE158284) and sixteen (GSE25631) sample outliers were removed from subsequent analyses. Quality control measures in the remaining datasets did not reveal any samples of poor quality.

Differential expression analysis
Differential expression analysis was performed using the limma package for microarray data and EdgeR for count-based data[37,38]. EnhancedVolcano was used to generate volcano plots of differentially expressed miRNA based on the log2 fold change ratio and false discovery-adjusted *P*-values (Benjamini-Hochberg)[43]. Differentially expressed miRNA hits were identified based on an adjusted *P*-value < 0.05 and log2 fold change

greater than or less than 1. Differential expression analysis results were integrated across datasets as following: an integrated meta log fold change value was summarized by the mean of all log fold changes across datasets using the MetaVolcano R package[44], whereas an integrated meta adjusted P-value was determined through a sample size-weighted Fisher's test using the metapro package[45]. miRNA differentially expressed across all datasets were ranked based on the index value which incorporates meta fold change and meta P-value. These results were visualized using the EnhancedVolcano[43] package and their certainty was assessed through literature review. For the leave-one-out validation, the integrated differential expression analysis was repeated nine times with each iteration excluding data from one specific dataset. Changes in significantly dysregulated hits were evaluated in comparison to the original list of hits.

Target prediction analysis

We identified 3 datasets which contain miRNA and protein-coding gene expression data for the same patient samples (GSE90598, GSE165286 and PDC000204). Unprocessed expression data was publicly available for GSE90598 and PDC000204. For GSE165286, raw fastq were processed using Salmon to generate transcript-level quantifications against a partial transcriptome index constructed from the Ensembl hg38 *Homo sapiens* reference genome (release 100)[46,47]. Quantified data were condensed to gene-level counts using the tximport package before conversion into an EdgeR-compatible dataset for analysis[48]. We performed platform-specific individual dataset processing, quality control, and differential expression analysis. These results were integrated using MetaVolcanoR and metapro packages as previously described. The list of dysregulated protein-coding genes was used for target prediction analysis.

Using the mirDIP tool, we conducted a bidirectional miRNA-target prediction between upregulated miRNA and downregulated protein-coding genes or downregulated miRNA and upregulated protein-coding genes[49]. The top 1% predicted interactions from mirDIP sources including miranda May 2021, RNA22, DIANA, mirDB v6 and TargetScan v7.2 were used for subsequent pathway profiling. Predictions identified across multiple mirDIP sources were filtered to create a list of unique miRNA-target interactions. These predictions were compared with experimentally validated interactions sourced from the DIANA-TarBase v9.0 and miR-TarBase v10.0 platforms[50,51].

Bootstrap analysis

Protein-coding genes were randomly bootstrap sampled without replacement over 1000 iterations using the python programming language. The number of genes sampled corresponded to the number of upregulated and downregulated protein-coding genes. A bidirectional miRNA-target prediction was performed for each set of randomized gene lists and the corresponding dysregulated miRNA list as described above using the mirDIP python API. The bootstrapped-based prediction analysis calculated the number of interactions between dysregulated miRNA and randomly sampled genes. Confidence intervals (CI) were calculated for each bootstrap sampled distribution to determine if the actual observed number of interactions identified was unique compared to the distribution of the number of random interactions.

Pathway analysis

We performed a hypergeometric enrichment test using the gProfiler g:GOSt pathway analysis tool[52]. The list of predicted upregulated and downregulated targets was ordered by confidence scores of miRNA-target interactions and was inputted into the gProfiler platform. The Reactome database was used to identify biological pathways associated with dysregulated targets. A network map was developed using the Cytoscape EnrichmentMap tool to visualize significant pathways with a g:SCS adjusted P-value threshold < 0.05[53]. Pathways were categorized using the Reactome pathway browser tool. Using gene lists associated with each pathway, dot plots were created to identify the predicted targets of miRNA implicated in ECM remodeling, growth, immune-related and core neuronal pathways.

Results

Largest collection of miRNA expression data from adult primary GBM

Our bioinformatics pipeline systematically acquired, processed, and analyzed individual GBM datasets to explore differential miRNA expression patterns (Fig. 1). We searched public repositories (NCBI GEO and NCI) for miRNA expression datasets meeting specific criteria, identifying 139 datasets. Given the distinct molecular and genetic profiles of adult and pediatric GBM, and thus differing disease mechanisms[54,55], our analysis focused solely on adult GBM. We filtered for datasets containing adult primary IDH-wildtype GBM samples with at least three tumor and three non-cancerous brain tissue controls, excluding recurrent, secondary, or IDH-mutant samples. Nine datasets including GSE158284, GSE109628, GSE90603, GSE65626, GSE25631, GSE91014 (TCGA), GSE165937, GSE214252, and PDC000204 met these criteria and were selected, irrespective of methodological and clinical variations (Table 1). Three datasets (GSE65626, GSE109628, GSE214252) contained patient-matched non-cancerous controls; whereas GSE90603 has partially matched samples. All profiling data originated from fresh-frozen brain samples, except for the PDC000204 controls, which were from post-mortem tissues. In total, our in-silico analysis comprises expression data from 743 adult GBM brain tissues and 59 non-cancerous brain controls.

To account for study heterogeneity, each of the nine datasets was processed and analyzed individually using appropriate tools for microarray, RNA sequencing, and Nanostring platforms. Stringent, platform-specific quality control measures were applied to ensure high-quality results. Five samples from GSE158284 and sixteen from GSE25631 were identified as low quality and removed from further analysis. Principal component analysis (PCA) visualization of the processed miRNA profiling data clearly distinguished non-cancerous brain tissues from GBM samples in most datasets (Fig. 2a–i).
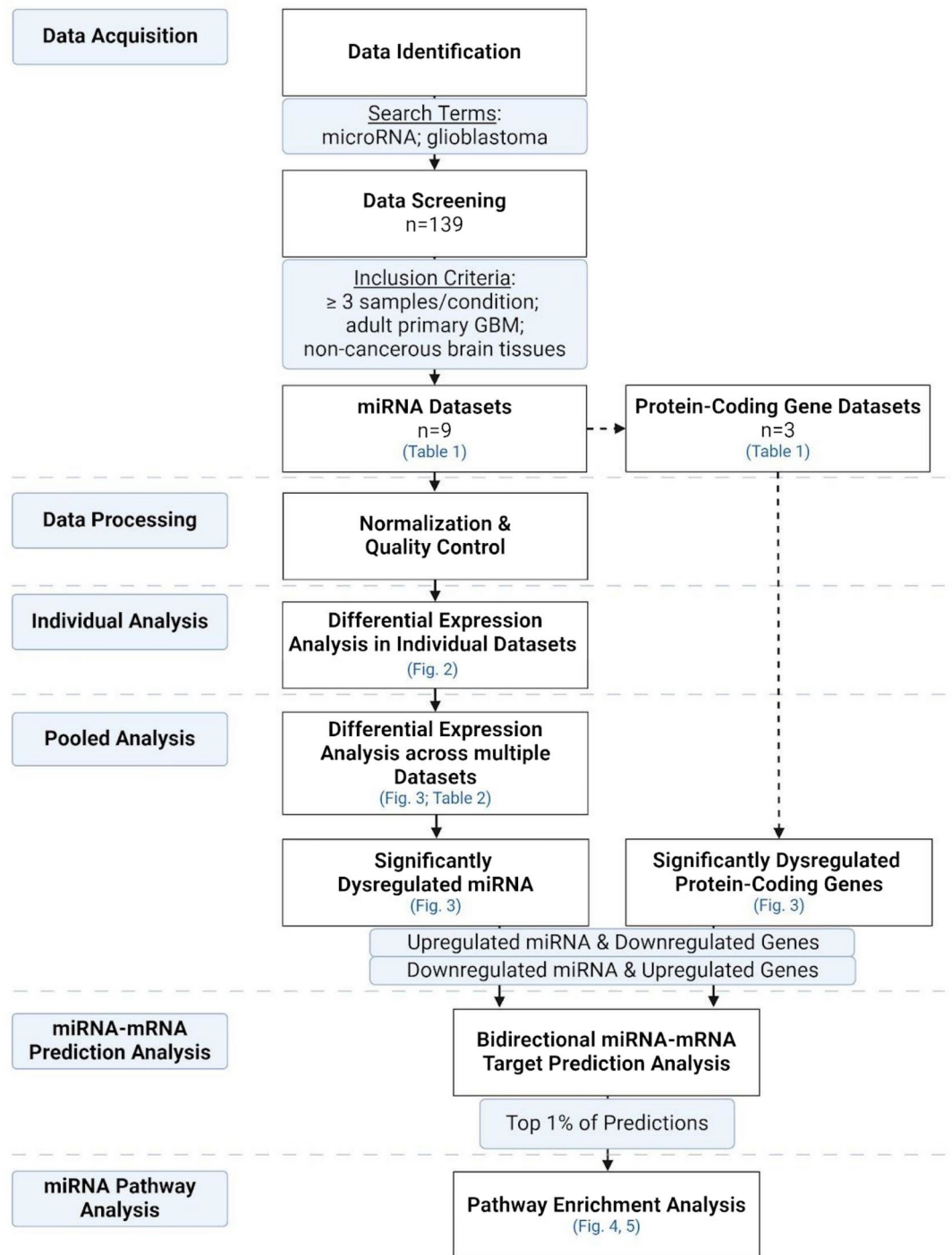
Fig. 1. Schematic overview of the miRNA analysis pipeline.

Differential expression analysis of integrated datasets identifies dysregulated miRNA in GBM

Differential expression analysis was performed individually on each dataset to identify dysregulated miRNA in GBM compared to controls (Fig. 2a–i). These results were then integrated using a weighted Fisher's test based on mean log fold change, revealing 209 significantly dysregulated miRNA (adjusted P-values < 0.05); 94 downregulated and 115 upregulated miRNA in GBM compared to non-cancerous brain tissues (Fig. 3a; Table 2; Supplementary Table S1). This list of widely dysregulated miRNA in GBM represents a valuable resource for future studies. Within these candidates, the top five downregulated miRNA were miR-139-5p, miR-124-3p, miR-128-3p, miR-7-5p, and miR-129-5p; the top five upregulated miRNA were miR-21-5p, miR-21-3p, miR-182-5p, miR-10a-5p, and miR-155-5p (Table 2; Supplementary Table S1).

Dataset ID	Sample size*		Age (mean ± SD)	Gender (F:M ratio)	Platform (miRNA)	Platform (protein-coding genes)	References
	GBM	Control					
GSE158284	17	10	63.8 (17.7)	4:13	Human miRNA Microarray (V3)	–	30
GSE109628	12	9#	69.6 (12.1)	4:8	Agilent-031181 Unrestricted_Human_miRNA_V16.0_Microarray	–	29
GSE90603	**16**	**7#**	**53.8 (17.0)**	**6:10**	**Affymetrix Multispecies miRNA-4 Array**	**Affymetrix Human Gene 2.1 ST Array**	28
GSE65626	3	3#	50 (8.54)	0:3	Affymetrix Multispecies miRNA-4 Array	–	–
GSE25631	62	5	46.72 (12.6)	21:41	Illumina Human v2 MicroRNA expression beadchip	–	26,27
GSE91014 (TCGA)	509	10	57.7 (13.9)	189:320	Agilent-016436 Human miRNA Microarray 1.0 G4472A	–	31
GSE165937	**9**	**4**	–	–	**Nanostring human miRNA panel (NS_H_MIR_V3A)**	**Illumina HiSeq 4000 (Homo sapiens)**	25
GSE214252	17	3#	–	–	Illumina HiSeq 4000 (Homo sapiens)	–	23
PDC000204	**98**	**8****	**58.7 (12.3)**	**42:56**	**Illumina HiSeq 4000 (Homo sapiens)**	**Illumina HiSeq 4000 (Homo sapiens)**	24

Table 1. Information regarding datasets identified to contain miRNA expression profiling data. Datasets that also include protein-coding gene profiling data are written in bold. Clinical information including age (mean ± SD) and gender (female:male ratio) is provided for GBM patients. *Sample size was calculated following filtering based on inclusion criteria and quality control analysis. **Control samples were obtained from post-mortem patients. #Datasets contain fully or partially matched control samples.

To assess the relative influence of each dataset on the overall analysis, we performed leave-one-out cross-validation by integrating differential expression analysis results from all datasets except one. Removing most datasets resulted in fewer than 6% change in the number of significant hits compared to the original list (Supplementary Table S2). The largest impact was observed when GSE158284 was removed, resulting in a 16.75% loss of significant hits (Supplementary Table S2). However, 83–99% of the significantly dysregulated hits remained consistent across all leave-one-out analyses, indicating that no single dataset unduly skewed the results.

Comprehensive analysis of miRNA-mediated mechanisms in GBM

To unravel the mechanisms underlying miRNA involvement in GBM progression, we investigated mRNA targets and pathways associated with the dysregulated miRNA identified in our analysis This involved integrating differential miRNA expression data, target prediction algorithms, protein-coding gene expression analysis, and pathway analysis (Fig. 1). This was performed using three datasets from our collection of nine, which also contained protein-coding gene expression profiling data (Table 1). Similar to the miRNA analysis pipeline, each dataset was processed and analyzed individually to account for methodological differences (Supplementary Fig. S2). Integrated differential expression analysis of protein-coding genes identified 1478 upregulated and 1189 downregulated genes in GBM compared to controls (Fig. 3b; Supplementary Table S3).

To integrate miRNA data with GBM expression data, we first proceeded with the basic assumption that miRNA are repressors of gene expression. Therefore, downregulated protein-coding genes were assessed for targeting by upregulated miRNA, and vice-versa. This analysis identified 603 putative target genes of the 115 upregulated miRNA, representing 1,902 unique miRNA-target interactions (Supplementary Table S4). Similarly, we identified 423 upregulated target genes of the 94 downregulated miRNA, representing 946 unique interactions (Supplementary Table S5).

To validate that the miRNA-target predictions were not due to chance, we used bootstrap sampling to generate random lists of protein-coding genes and then identified miRNA-target interactions between these random gene sets and the dysregulated miRNA. Using the mirDIP software, we identified 4587 (95% CI 3978–5224) and 4535 (95% CI 4054–5084) interactions between the upregulated miRNA and 1,189 random genes, and the downregulated miRNA and 1478 random genes, respectively (Supplementary Fig. S3). In contrast, our actual number of interactions was 2948 and 1902, respectively (Supplementary Fig. S3). Because the observed number of interactions exceeded the 95% confidence interval of the random distribution, this analysis demonstrates that the identified miRNA-target interactions are non-random.

To further validate our predictions, we compared our findings to experimentally validated miRNA-mRNA interactions from the DIANA-TarBase and miRTarBase databases We found that 500 of 1902 (26.29%) upregulated miRNA–downregulated target interactions and 180 of 946 (19.02%) downregulated miRNA–upregulated target interactions were experimentally validated in either miRTarBase or DIANA-TarBase (Supplementary Fig. S4, Supplementary Tables S4, S5). While most interactions remain unstudied, the presence of these experimentally validated interactions strengthens our findings.

miRNA are associated with ECM remodeling genes in GBM

To explore the molecular mechanisms by which dysregulated miRNA contribute to GBM pathogenesis, we performed functional pathway enrichment analysis on the predicted miRNA-target interactions using gProfiler. Analysis of pathways associated with upregulated genes targeted by downregulated miRNA revealed significant enrichment in 25 Reactome pathways, including ECM organization and growth signaling (adjusted
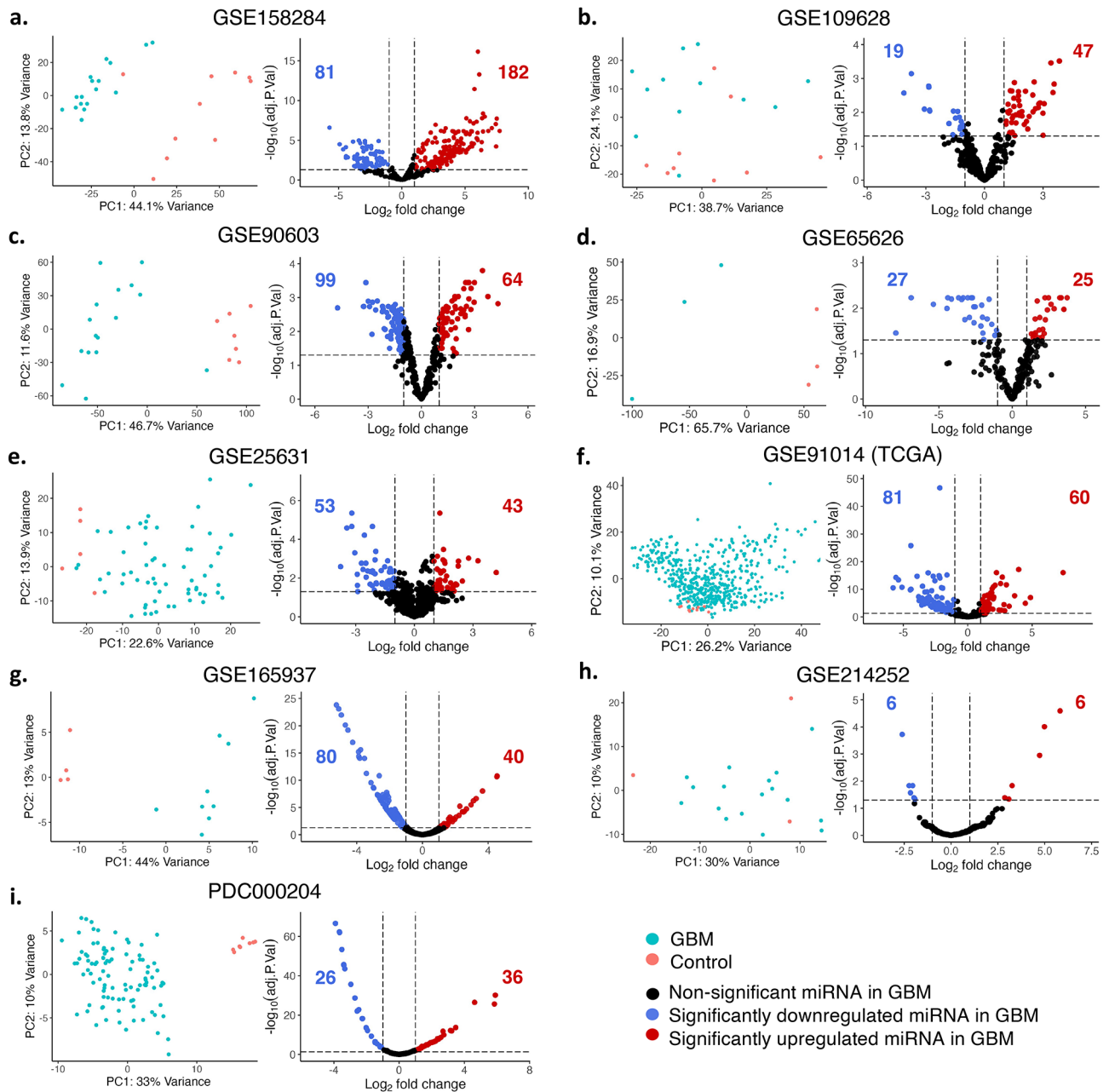
Fig. 2. PCA and volcano plots identify differences in miRNA expression between GBM and controls in nine datasets. Each panel highlights data from one dataset: GSE158284 (**a**), GSE109628 (**b**), GSE90603 (**c**), GSE65626 (**d**), GSE25631 (**e**), GSE91014 (TCGA) (**f**), GSE165937 (**g**), GSE214252 (**h**) and PDC000204 (**i**). Left side of each panel shows PCA clustering based on miRNA expression data, with GBM brain samples in light blue and non-cancerous brain samples in light red. On the right side, volcano plots illustrate differentially expressed miRNA. Total number of significantly dysregulated hits in GBM (q-value < 0.05, log2 fold change > 1) is noted for each dataset. Significantly upregulated miRNA are highlighted in dark red, while downregulated miRNA are in dark blue.

$p < 0.05$) (Fig. 4a; Supplementary Table S6). The ECM organization pathway showed the most significant enrichment (adjusted $p < 0.0001$), with other ECM-related pathways also highly ranked. Further investigation of downregulated miRNA targeting upregulated ECM-related genes (Fig. 4b) revealed four enriched collagen organization pathways (Fig. 4a). miR-29b-3p and miR-29c-3p were identified to target *COL1A2*, *COL3A1*, *COL5A1* and *COL6A3*, suggesting that they may be regulators of collagen expression. Further interactions with collagen-associated genes was predicted to occur through miR-521, miR-7-5p, miR-628-5p, and miR-4443 by targeting *COL4A6*, *COL1A2*, *COL4A1*, and *COL5A1*, respectively. Additionally, we identified miR-29b-3p and miR-29c-3p to target *LAMC1*, and miR-1182 to target *LAMC2*, two genes encoding for laminin, a class of crucial ECM proteins. Additional ECM-regulating miRNA include miR-638, which targets *BCAN*, a gene
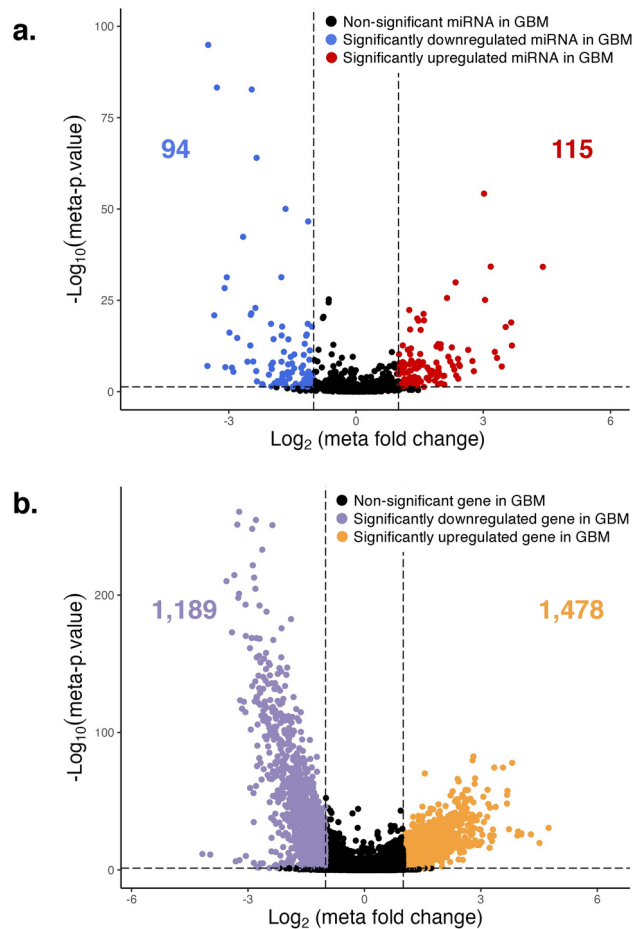
Fig. 3. Identification of miRNA and protein-coding genes widely dysregulated in GBM. Volcano plot illustrating dysregulated miRNA (**a**) and protein-coding genes (**b**) in GBM across all 9 and 3 datasets, respectively. Total number of significantly dysregulated hits in GBM (q-value < 0.05, log2 fold change > 1) is noted for plot. Significantly upregulated genes are highlighted in red (**a**) and orange (**b**), while downregulated genes are in blue (**a**) and purple (**b**).

that encodes a member of the lectican family of chondroitin sulfate proteoglycans specifically expressed in the brain[56]. miR-218-5p targets *TNC,* a gene that encodes a protein that contains multiple EGF-like and fibronectin type-III domains implicated in guidance of migrating neurons as well as axons during development, synaptic plasticity, and neuronal regeneration[57]. miR-218-5p also targets *FBN2*, which encodes for a component of connective tissue microfibrils and may be involved in elastic fiber assembly[58]. Furthermore, we discovered three miRNA implicated in ECM degradation by regulating MMPs, including miR-1225-5p and miR-485-5p targeting *MMP14*, and miR-3200-5p targeting *MMP19.* In summary, we identified several downregulated miRNA in GBM that regulate genes involved in ECM organization, primarily through the regulation of collagen formation and degradation. The dysregulation of miR-29b-3p and miR-29c-3p, with their predicted targeting of multiple collagen-related genes, suggests a significant impact on collagen networks within the GBM ECM.

miRNA influence on growth- and immune-related pathways in GBM
Our pathway analysis also revealed significant associations between downregulated miRNA and their upregulated targets within growth factor and immune signaling pathways. Specifically, we identified associations with nine receptor tyrosine kinase-related pathways and three interleukin-related signaling pathways (Fig. 4a). Further investigation of downregulated miRNA and their predicted upregulated target genes (Fig. 4c) showed that miR-29b-3p and miR-29c-3p target *VEGFA*, miR-7-5p targets *EGFR*, and miR-149-5p, miR-218-5p, and miR-219a-5p target *PDGFRA*—key receptor tyrosine kinases implicated in GBM development[59]. Additionally, miR-132-3p targets *HBEGF* and *EGF1*, miR-139-5p targets *FOS* and *JUN*, and miR-149-5p and miR-218-5p target *TCF12*, all of which are involved in tumor progression[60–64].

Our results also implicate the involvement of miRNA in cytokine signaling in GBM. We identified several downregulated miRNA associated with factors that recruit tumor-associated macrophages, including miR-346 (targeting *LIF* and *OAS2*) and miR-1229-3p (targeting *CCR5*)[65–67]. Several miRNA were also implicated in tumor necrosis factor signaling, such as miR-495-3p (targeting *TNFRSF1B*) and miR-330-5p and miR-326 (targeting *TNFSF14*). Additionally, we identified miRNA that regulate downstream mediators of cytokine

Downregulated miRNA				Upregulated miRNA			
hsa-miR-139-5p	hsa-miR-127-3p	hsa-miR-495-3p	hsa-miR-575	hsa-miR-21-5p	hsa-miR-199b-5p	hsa-miR-1539	hsa-miR-595
hsa-miR-124-3p	hsa-miR-149-5p	hsa-miR-138-1-3p	hsa-miR-2861	hsa-miR-21-3p	hsa-miR-301b-3p	hsa-miR-532-3p	hsa-miR-8084
hsa-miR-128-3p	hsa-miR-432-5p	hsa-miR-6743-5p	hsa-miR-4253	hsa-miR-182-5p	hsa-miR-373-5p	hsa-miR-106a-5p	hsa-miR-502-3p
hsa-miR-7-5p	hsa-miR-29c-3p	hsa-miR-760	hsa-miR-765	hsa-miR-10a-5p	hsa-miR-17-3p	hsa-miR-17-5p	hsa-miR-214-3p
hsa-miR-129-5p	hsa-miR-338-5p	hsa-miR-328-3p	hsa-miR-758-5p	hsa-miR-155-5p	hsa-miR-183-5p	hsa-miR-18b-5p	hsa-miR-10b-3p
hsa-miR-137-3p	hsa-miR-490-3p	hsa-miR-3200-5p	hsa-miR-936	hsa-miR-10b-5p	hsa-miR-130a-3p	hsa-miR-551b-3p	hsa-miR-144-3p
hsa-miR-218-5p	hsa-miR-487b-3p	hsa-miR-642a-5p	hsa-miR-6511a-3p	hsa-miR-196b-5p	hsa-miR-199a-3p	hsa-miR-337-5p	hsa-miR-146b-5p
hsa-miR-769-5p	hsa-miR-138-5p	hsa-miR-149-3p		hsa-miR-210-3p	hsa-miR-20a-5p	hsa-miR-590-5p	hsa-miR-32-5p
hsa-miR-139-3p	hsa-miR-656-3p	hsa-miR-4443		hsa-miR-196a-5p	hsa-miR-450a-5p	hsa-miR-223-3p	hsa-miR-454-3p
hsa-miR-323a-3p	hsa-miR-338-3p	hsa-miR-513a-3p		hsa-miR-199b-3p	hsa-miR-23a-3p	hsa-miR-483-3p	hsa-miR-93-3p
hsa-miR-330-3p	hsa-miR-323a-5p	hsa-miR-129-1-3p		hsa-miR-106b-5p	hsa-miR-1246	hsa-miR-34a-5p	hsa-miR-215-5p
hsa-miR-433-3p	hsa-miR-410-3p	hsa-miR-1288-3p		hsa-miR-27a-3p	hsa-miR-503-5p	hsa-miR-19a-3p	hsa-miR-505-3p
hsa-miR-448	hsa-miR-1224-5p	hsa-miR-1182		hsa-miR-135b-5p	hsa-miR-362-3p	hsa-miR-545-3p	hsa-miR-15b-3p
hsa-miR-129-2-3p	hsa-miR-29b-3p	hsa-miR-876-3p		hsa-miR-20a-3p	hsa-miR-362-5p	hsa-miR-181a-2-3p	hsa-miR-450b-5p
hsa-miR-504-5p	hsa-miR-485-5p	hsa-miR-330-5p		hsa-miR-93-5p	hsa-miR-142-3p	hsa-miR-629-3p/5p	hsa-miR-376b-3p
hsa-miR-203a-3p	hsa-miR-885-5p	hsa-miR-770-5p		hsa-miR-15b-5p	hsa-miR-542-5p	hsa-miR-550a-3p/5p	hsa-miR-30b-3p
hsa-miR-491-5p	hsa-miR-485-3p	hsa-miR-892b		hsa-miR-25-3p	hsa-miR-532-5p	hsa-miR-339-3p	hsa-miR-431-5p
hsa-miR-383-5p	hsa-miR-1229-3p	hsa-miR-1225-5p		hsa-miR-193a-3p	hsa-miR-16-2-3p	hsa-miR-106b-3p	hsa-miR-3651
hsa-miR-12136	hsa-miR-769-3p	hsa-miR-1914-3p		hsa-miR-1825	hsa-miR-424-3p	hsa-miR-660-5p	hsa-miR-374b-3p
hsa-miR-517c-3p	hsa-miR-326	hsa-miR-596		hsa-miR-339-5p	hsa-miR-424-5p	hsa-miR-629-3p	hsa-miR-629-5p
hsa-miR-874-3p	hsa-miR-1296-5p	hsa-miR-1275		hsa-miR-130b-3p	hsa-miR-34a-3p	hsa-miR-877-3p	hsa-let-7a-3p
hsa-miR-138-2-3p	hsa-miR-577	hsa-miR-636		hsa-miR-455-3p	hsa-miR-16-5p	hsa-miR-615-3p	hsa-miR-30d-3p
hsa-miR-628-3p	hsa-miR-628-5p	hsa-miR-1185-5p		hsa-miR-96-5p	hsa-miR-148a-3p	hsa-miR-602	hsa-miR-654-3p
hsa-miR-132-3p	hsa-miR-105-5p	hsa-miR-638		hsa-miR-224-5p	hsa-miR-199a-5p	hsa-miR-320e	hsa-miR-144-5p
hsa-miR-873-5p	hsa-miR-521	hsa-miR-187-5p		hsa-miR-142-5p	hsa-miR-1290	hsa-let-7i-3p	hsa-miR-937-3p
hsa-miR-219a-2-3p	hsa-miR-346	hsa-miR-487a-5p		hsa-miR-92b-3p	hsa-miR-455-5p	hsa-miR-99a-3p	hsa-miR-550b-2-5p
hsa-miR-522-3p	hsa-miR-1250-5p	hsa-miR-668-3p		hsa-miR-550a-3p	hsa-miR-500a-3p	hsa-miR-423-3p	hsa-miR-1537-3p
hsa-miR-375-3p	hsa-miR-889-3p	hsa-miR-3131		hsa-miR-18a-5p	hsa-miR-195-3p	hsa-miR-1910-5p	hsa-miR-378f
hsa-miR-329-3p	hsa-miR-219a-5p	hsa-miR-3200-3p		hsa-miR-542-3p	hsa-miR-20b-5p	hsa-miR-296-5p	

Table 2. List of significantly downregulated and upregulated miRNA across all datasets in GBM. All hits highlighted have a meta P-value < 0.05 and meta fold change > 1. Significant miRNA hits are ranked based on their index score which incorporates meta P-value and meta fold change.

signaling, including miR-139-5p and miR-936 (targeting *SOCS2*) and miR-2861 (targeting *SOCS3*), family members previously linked to increased immune cell infiltration in GBM[68]. In summary, our findings highlight a set of downregulated miRNA predicted to regulate upregulated mRNA encoding crucial growth and immune-related signaling molecules in GBM.

miRNA regulation of neuronal processes in GBM

Finally, we performed pathway enrichment analysis to investigate the molecular role of the downregulated predicted targets of upregulated miRNA hits. Conversely, we determined that upregulated miRNA and their predicted downregulated targets are significantly associated with 35 Reactome pathways (adjusted P-values < 0.05), predominantly reflecting core neuronal processes highlighted by their association with nine neurotransmitter release cycle, two receptor activation and two synapse interaction pathways (Fig. 5a, Supplementary Table S5). To examine their specific roles, we identified predicted targets of several dysregulated miRNA candidates involved in synaptic-related pathways (Fig. 5b). Our analysis identified miRNA that target key genes involved in governing vesicular trafficking and exocytosis during synaptic release, comprising miR-10b-3p, miR-34a-5p, miR-193a-3p targeting *SYT1*, miR-135b-5p targeting *CPLX2*, and miR-337-5p targeting *VAMP2*. Our results also implicate miRNA in synaptic formation through regulation of neurexins, including miR-455-3p, miR-10b-3p which target *NRXN1* and miR-595 which targets *NRXN3*. In addition to regulators of synaptic function across multiple neurotransmitters, our analysis identified miRNA that specifically disrupt glutamatergic signaling through miR-10b-3p targeting *GRIN2A*, miR-34a-5p targeting *GRM7*, miR-455-3p targeting *SLC1A2*, and miR-20b-5p targeting *SLC17A7*. GABAergic signaling was also subject to miRNA control through miR-34a-5p targeting *GABRA3*, miR-10a-5p targeting *GABRB2*, and miR-376b-3p targeting *SLC6A1*. Overall, we identified upregulation of multiple miRNA with predicted roles in neuronal activity and synaptic communication.
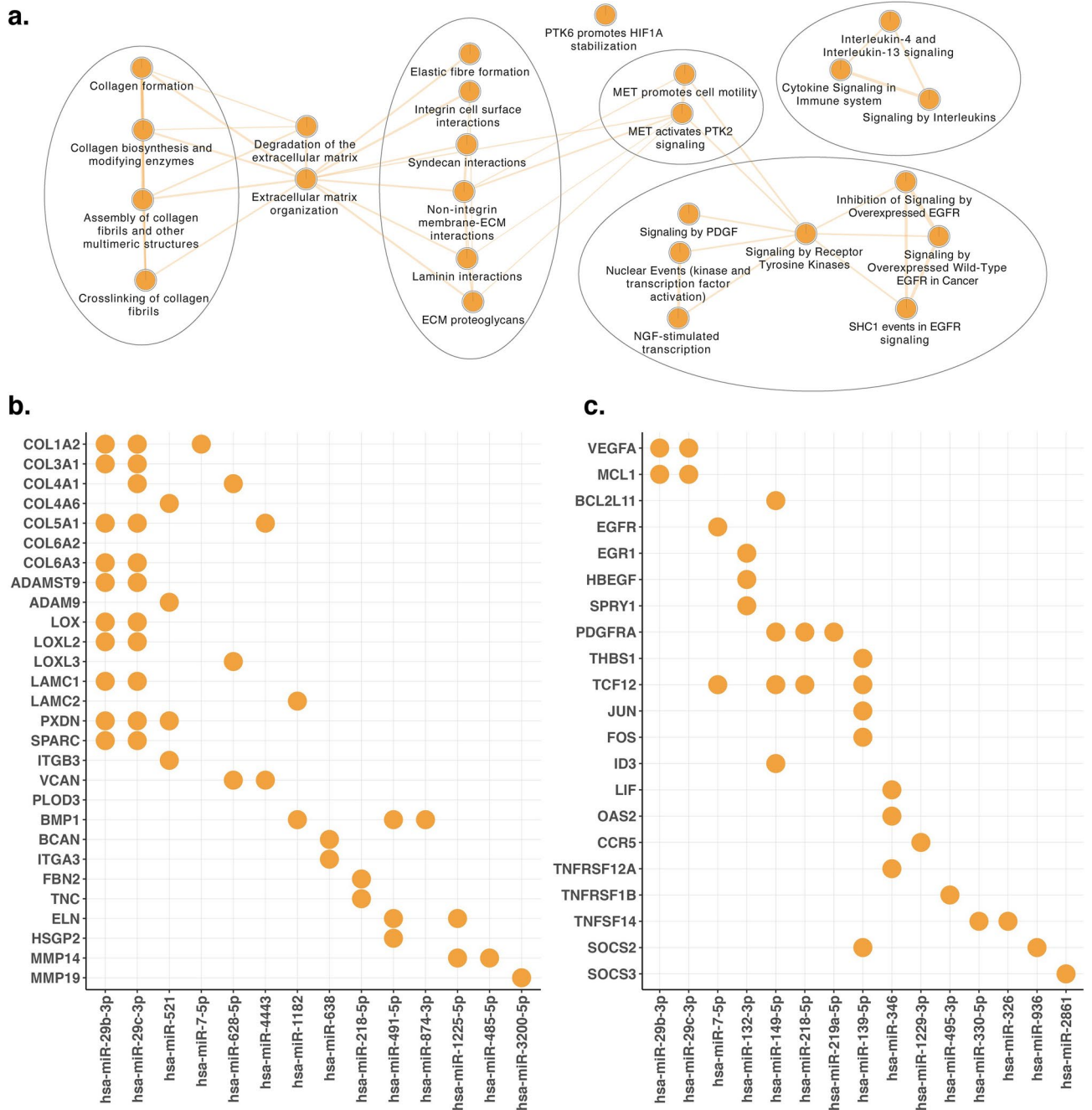
Fig. 4. Pathways linked with downregulated miRNA hits showcase their involvement in ECM remodeling, growth, and immune-related signaling. (**a**) Network map of pathway enrichment analysis from upregulated genes targeted by downregulated miRNA. (**b**) Dot plot revealing targets of candidate downregulated miRNA associated with ECM remodeling pathways. (**c**) Dot plot revealing targets of candidate downregulated miRNA associated with growth-stimulating and immune-related signaling pathways.

Discussion

Many miRNA linked to GBM progression have been studied, but most remain unexplored due to outdated and low-quality expression data, particularly from microarray platforms. By integrating available datasets, we created the largest-to-date collection of miRNA expression data from adult primary GBM patients, providing the most comprehensive analysis of miRNA in GBM to date. To our knowledge, this study uses the largest collection of GBM miRNA expression data, encompassing 743 GBM tissues and 59 non-cancerous brain controls. Only two previous studies have reported on miRNA expression in both adult and pediatric GBM samples. Wang and Lu examined miRNA expression profiles in 125 brain and 207 serum samples from GBM patients[32], while Bayat and colleagues investigated microarray datasets from 670 GBM patients[33]. In contrast, our analysis incorporates
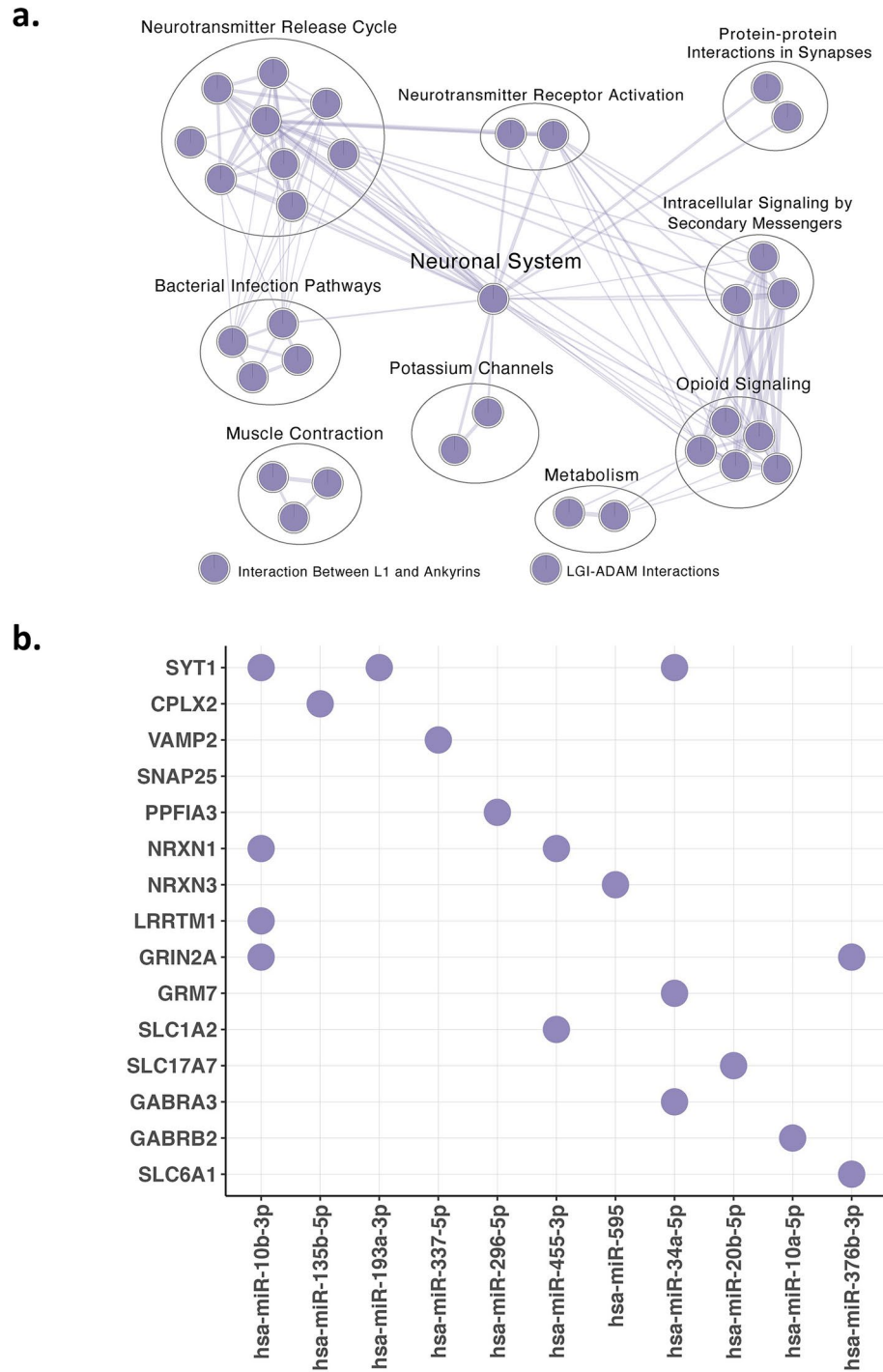
Fig. 5. Pathways linked with upregulated miRNA hits highlight their involvement in core neuronal processes. (**a**) Network map of pathway enrichment analysis from downregulated genes targeted by upregulated miRNA. (**b**) Dot plot revealing targets of candidate upregulated miRNA associated with core neuronal pathways.

additional profiling data and is exclusively focused on carefully curated datasets of adult primary GBM tumors. Stringent quality control measures were implemented to ensure data integrity and eliminate low-quality samples.

However, our analysis is not without limitations. The use of microarray data, which does not capture the full spectrum of miRNA expression, limited the number of miRNA analyzed across all datasets after filtering out low-expression miRNA. This limitation highlights the need for future high-throughput profiling of miRNA in GBM. Another limitation was the integration of data from various platforms. To address this, we performed leave-one-out cross-validation, demonstrating that no single dataset unduly influenced the results, thereby supporting the feasibility of our integrated approach. Integrating the differential expression analysis results from all nine datasets allowed the identification of consistently dysregulated miRNA across multiple studies.

Furthermore, Our integrated analysis, using a weighted Fisher's test, identified 94 significantly downregulated and 115 significantly upregulated miRNA in adult primary GBM compared to non-cancerous brain tissue. Among the dysregulated miRNA, several have been previously associated with GBM pathogenesis. For instance, the upregulated miR-21 and miR-10b are reported to contribute to GBM tumour growth in vitro and in vivo[33,69]. Similarly, downregulated hits including miR-139 and miR-124 are reported to have tumor suppressive functions in GBM[70,71]. The identification of these previously characterized miRNA strengthens the confidence in our methodology and findings.

We also identified several downregulated miRNA with no reported link to GBM (miR-12136, miR-323a-5p, miR-521, miR-1250-5p, miR-642a-5p) and several that have been linked to GBM (miR-874-3p, miR-628-3p, miR-219a-2-3p, miR-487-3p, miR-885-5p, miR-628-5p, miR-889-3p, miR-6743-5p), but specific roles have not been investigated. Similarly, we identified upregulated miRNA not previously reported as dysregulated in GBM (miR-199b-5p, miR-500a-3p, miR-1539, miR-660-5p) and a subset with uncharacterized roles (miR-1825, miR-550a-3p, miR-551b-3p, miR-590-5p, miR-337-5p, miR-339-3p, miR-595, miR-602, miR-320e, miR-877-3p) are also identified. Importantly, the increased statistical power afforded by our larger sample size enabled the identification of miRNA not previously investigated in GBM, opening avenues for novel discoveries and potentially revealing previously unknown regulatory mechanisms in GBM biology.

To investigate potential mechanisms underlying the roles of these miRNA in GBM development, we next examined the targetome of all dysregulated miRNA. Because miRNA target prediction algorithms often fail to account for tissue-specific differences in gene expression and miRNA-mRNA interactions, we integrated miRNA prediction algorithms with differential expression analysis of protein-coding genes, focusing on dysregulated miRNA and protein-coding genes with reciprocally directed expression changes.

This analysis revealed strong associations between miRNA dysregulation and gene networks involved in ECM organization. The normal brain ECM is characterized by a low-stiffness composition, dominated by hyaluronan, glycosaminoglycans, and proteoglycans[72,73]. However, ECM remodeling, leading to a denser, stiffer matrix, promotes aggressive cell invasion[74,75]. This remodeling process involves ECM degradation by matrix metallopeptidases (MMPs)[76,77] and the secretion of fibrous components such as collagen, laminin, and fibronectin[78,79]. Altered ECM composition modifies tumor biomechanics, promoting treatment resistance by influencing proliferation, invasion, migration, and survival[74,79]. In our analysis, miR-29b-3p and miR-29c-3p emerged as key miRNA predicted to target multiple ECM genes. Interestingly, we found that miR-218-3p mediates ECM remodeling by regulating *TNC*, a role previously shown to promote GBM progression[80]. The remaining predicted interactions are novel in the context of GBM and suggest a key role for miRNA in overall ECM composition. Dysregulation of these miRNA in GBM is hypothesized to alter the tumor microenvironment (TME), enhancing GBM progression and invasiveness. This is supported by studies showing that increased collagen or laminin levels correlate with more aggressive GBM phenotypes[81,82]. Specifically, collagen promotes GBM cell mobility and metastasis[83–85] potentially through destabilization of cell polarity and cell–cell adhesion, and stimulation of growth factor signaling[86]. Therefore, downregulation of these miRNA is predicted to derepress ECM components, particularly collagen, and promote GBM invasiveness. Overall, our results highlight the importance of understanding miRNA-mediated mechanisms regulating ECM in GBM.

We also identified several downregulated miRNA predicted to regulate growth factor and immune-related signaling. While most of these interactions are novel in the context of GBM, our analysis did reveal several bonafide miRNA-target interactions including miR-7-5p with EGFR[87], miR-218-5p with PDGFRA[88], and TCF12[89] which instill confidence on our findings. Our analysis suggests that miRNA dysregulation may influence key aspects of GBM aggressiveness. Firstly, we propose that miRNA are associated with GBM through the regulation of key pathways involved in disease progression, including VEGFA, EGFR, PDGFRA signaling[59]. Although these pathways are commonly upregulated in GBM and associated with aggressive phenotypes, the role of miRNA in these processes is not well understood. Second, our study suggests a potential role for miRNA in regulating the recruitment of pro-tumoral immune cells through targeting components of cytokine signaling, including *LIF* and *OAS2*[65,66]. These findings implicate miRNA in immune cell infiltration, TME remodeling, and GBM progression, consistent with previous studies demonstrating that specific miRNA mediate the recruitment and activation of tumor-associated immune cells[90,91].

We also identified multiple miRNA predicted to regulate genes crucial for neuronal activity, particularly synaptic communication. The reliability of our prediction pipeline is supported by the identification of the previously reported and experimentally validated interaction between miR-34a-5p and *GRM7*[92]. The association of these neuronal pathways with mature neurons suggests that our analysis may reflect a decreased proportion of mature neurons in GBM compared to non-cancerous brain controls. Because tissue specimens are typically bulk samples, several factors could contribute to the observed lower levels of neuronal processes. These include a lower proportion of mature neurons and the presence of dedifferentiated GBM cells, which, while shown to communicate with surrounding brain tissue and integrate into neural circuits to promote aggressiveness, only form functional synapses with surrounding mature neurons in approximately 10% of cases[10,93–95]. The presence of other cancer-associated cells, such as immune cells, may further contribute to the observed relative decrease in neuronal processes.

In conclusion, this study provides a valuable resource describing the landscape of miRNA expression in GBM and highlights the need for large-scale, miRNA-focused clinical studies to further elucidate the roles of all miRNA in this disease. Despite limitations in current datasets, we have identified numerous dysregulated miRNA warranting further investigation as potential therapeutic targets. The potential role of miRNA in promoting GBM aggressiveness by reshaping the TME is particularly intriguing and represents a promising avenue for therapeutic exploration. These findings, coupled with the recent excitement surrounding the Nobel Prize awarded for miRNA discovery, generate novel hypotheses regarding miRNA regulation in GBM biology,

suggesting innovative miRNA-targeted therapeutic strategies[34]. Advancements in RNA and RNAi therapeutics further enhance the potential of miRNA-based therapies for GBM[96].

Data availability
The data that support the findings of this study are available from the corresponding author upon request.

References
1. Louis, D. N. et al. The 2021 WHO classification of tumors of the central nervous system: A summary. *Neuro Oncol.* **23**, 1231–1251 (2021).
2. Ostrom, Q. T. et al. CBTRUS statistical report: Primary brain and other central nervous system tumors diagnosed in the United States in 2015–2019. *Neuro Oncol.* **24**, v1–v95 (2022).
3. Gerritsen, J. K. W. et al. Safe surgery for glioblastoma: Recent advances and modern challenges. *Neurooncol Pract* **9**, 364–379 (2022).
4. Chen, J. et al. A restricted cell population propagates glioblastoma growth after chemotherapy. *Nature* **488**, 522–526 (2012).
5. Bao, S. et al. Glioma stem cells promote radioresistance by preferential activation of the DNA damage response. *Nature* **444**, 756–760 (2006).
6. Richards, L. M. et al. Gradient of developmental and injury response transcriptional states defines functional vulnerabilities underpinning glioblastoma heterogeneity. *Nat. Cancer* **2**, 157–173 (2021).
7. Couturier, C. P. et al. Single-cell RNA-seq reveals that glioblastoma recapitulates a normal neurodevelopmental hierarchy. *Nat. Commun.* **11**, 3406 (2020).
8. Wang, Q. et al. Tumor evolution of glioma-intrinsic gene expression subtypes associates with immunological changes in the microenvironment. *Cancer Cell* **32**, 42-56.e6 (2017).
9. Jain, S. *et al.* Single-cell RNA sequencing and spatial transcriptomics reveal cancer-associated fibroblasts in glioblastoma with protumoral effects. *J. Clin. Invest.* **133**, (2023).
10. Krishna, S. et al. Glioblastoma remodelling of human neural circuits decreases survival. *Nature* **617**, 599–607 (2023).
11. Yeo, A. T. et al. Single-cell RNA sequencing reveals evolution of immune landscape during glioblastoma progression. *Nat. Immunol.* **23**, 971–984 (2022).
12. Desland, F. A. & Hormigo, A. The CNS and the brain tumor microenvironment: implications for glioblastoma immunotherapy. *Int. J. Mol. Sci.* **21**, (2020).
13. Markovic, D. S., Glass, R., Synowitz, M., van Rooijen, N. & Kettenmann, H. Microglia stimulate the invasiveness of glioma cells by increasing the activity of metalloprotease-2. *J. Neuropathol. Exp. Neurol.* **64**, 754–762 (2005).
14. Galbo, P. M. et al. Functional contribution and clinical implication of cancer-associated fibroblasts in glioblastoma. *Clin. Cancer Res.* **30**, 865–876 (2024).
15. Friedman, R. C., Farh, K.K.-H., Burge, C. B. & Bartel, D. P. Most mammalian mRNAs are conserved targets of microRNAs. *Genome Res.* **19**, 92–105 (2009).
16. Zeng, Y., Yi, R. & Cullen, B. R. MicroRNAs and small interfering RNAs can inhibit mRNA expression by similar mechanisms. *Proc. Natl. Acad. Sci. USA* **100**, 9779–9784 (2003).
17. Bartel, D. P. Metazoan MicroRNAs. *Cell* **173**, 20–51 (2018).
18. Zeng, Y., Wagner, E. J. & Cullen, B. R. Both natural and designed micro RNAs can inhibit the expression of cognate mRNAs when expressed in human cells. *Mol. Cell* **9**, 1327–1333 (2002).
19. Barzegar Behrooz, A. et al. Integrating multi-omics analysis for enhanced diagnosis and treatment of glioblastoma: A comprehensive data-driven approach. *Cancers (Basel)* **15**, (2023).
20. Sana, J. et al. Risk Score based on microRNA expression signature is independent prognostic classifier of glioblastoma patients. *Carcinogenesis* **35**, 2756–2762 (2014).
21. Kouri, F. M. et al. miR-182 integrates apoptosis, growth, and differentiation programs in glioblastoma. *Genes Dev.* **29**, 732–745 (2015).
22. de la Rocha, A. M. A. et al. miR-425-5p, a SOX2 target, regulates the expression of FOXJ3 and RAB31 and promotes the survival of GSCs. *Arch. Clin. Biomed. Res.* **4**, 221–238 (2020).
23. Sallam, M. *et al.* Meta-Analysis of RNA-Seq Datasets Identifies Novel Players in Glioblastoma. *Cancers (Basel)* **14**, (2022).
24. Wang, L.-B. et al. Proteogenomic and metabolomic characterization of human glioblastoma. *Cancer Cell* **39**, 509-528.e20 (2021).
25. Yeh, M. et al. MicroRNA-138 suppresses glioblastoma proliferation through downregulation of CD44. *Sci. Rep.* **11**, 9219 (2021).
26. Chen, L. et al. The putative tumor suppressor miR-524-5p directly targets Jagged-1 and Hes-1 in glioma. *Carcinogenesis* **33**, 2276–2282 (2012).
27. Zhang, W. et al. miR-181d: A predictive glioblastoma biomarker that downregulates MGMT expression. *Neuro Oncol.* **14**, 712–719 (2012).
28. Gulluoglu, S. et al. Simultaneous miRNA and mRNA transcriptome profiling of glioblastoma samples reveals a novel set of OncomiR candidates and their target genes. *Brain Res.* **1700**, 199–210 (2018).
29. Hide, T. et al. Oligodendrocyte progenitor cells and macrophages/microglia produce glioma stem cell niches at the tumor border. *EBioMedicine* **30**, 94–104 (2018).
30. Junior, L. G. D. et al. High-throughput microRNA profile in adult and pediatric primary glioblastomas: The role of miR-10b-5p and miR-630 in the tumor aggressiveness. *Mol. Biol. Rep.* **47**, 6949–6959 (2020).
31. Brennan, C. W. et al. The somatic genomic landscape of glioblastoma. *Cell* **155**, 462–477 (2013).
32. Wang, W.-Y. & Lu, W.-C. Reduced expression of hsa-miR-338-3p contributes to the development of glioma cells by targeting mitochondrial 3-Oxoacyl-ACP synthase (OXSM) in glioblastoma (GBM). *Onco Targets Ther.* **13**, 9513–9523 (2020).
33. Bayat, H., Pourgholami, M. H., Rahmani, S., Pournajaf, S. & Mowla, S. J. Synthetic miR-21 decoy circularized by tRNA splicing mechanism inhibited tumorigenesis in glioblastoma in vitro and in vivo models. *Mol. Ther. Nucleic Acids* **32**, 432–444 (2023).
34. Ledford, H. MicroRNAs won the Nobel - will they ever be useful as medicines?. *Nature* https://doi.org/10.1038/d41586-024-03303-7 (2024).
35. Lopez-Romero, P. AgiMicroRna: Processing and differential expression analysis of agilent microRNA chips. *Bioconductor* https://doi.org/10.18129/b9.bioc.agimicrorna (2023).
36. Carvalho, B. S. & Irizarry, R. A. A framework for oligonucleotide microarray preprocessing. *Bioinformatics* **26**, 2363–2367 (2010).
37. Ritchie, M. E. et al. limma powers differential expression analyses for RNA-sequencing and microarray studies. *Nucleic Acids Res.* **43**, e47 (2015).
38. Robinson, M. D., McCarthy, D. J. & Smyth, G. K. edgeR: a Bioconductor package for differential expression analysis of digital gene expression data. *Bioinformatics* **26**, 139–140 (2010).

39. Shi, W., Oshlack, A. & Smyth, G. K. Optimizing the noise versus bias trade-off for Illumina whole genome expression BeadChips. *Nucleic Acids Res.* **38**, e204 (2010).
40. Ritchie, M. E. et al. A comparison of background correction methods for two-colour microarrays. *Bioinformatics* **23**, 2700–2707 (2007).
41. Xu, T. et al. miRBaseConverter: an R/Bioconductor package for converting and retrieving miRNA name, accession, sequence and family information in different versions of miRBase. *BMC Bioinformatics* **19**, 514 (2018).
42. Kauffmann, A., Gentleman, R. & Huber, W. arrayQualityMetrics–a bioconductor package for quality assessment of microarray data. *Bioinformatics* **25**, 415–416 (2009).
43. Blighe, K., Rana, S. & Lewis, M. EnhancedVolcano: Publication-ready volcano plots with enhanced colouring andlabeling. *Bioconductor* https://doi.org/10.18129/b9.bioc.enhancedvolcano (2022).
44. Prada, C., Lima, D. & Nakaya, H. MetaVolcanoR: Gene expression meta-analysis visualization tool. *Bioconductor* https://doi.org/10.18129/b9.bioc.metavolcanor (2022).
45. Yoon, S., Baik, B., Park, T. & Nam, D. Powerful p-value combination methods to detect incomplete association. *Sci. Rep.* **11**, 6980 (2021).
46. Patro, R., Duggal, G., Love, M. I., Irizarry, R. A. & Kingsford, C. Salmon provides fast and bias-aware quantification of transcript expression. *Nat. Methods* **14**, 417–419 (2017).
47. Martin, F. J. et al. Ensembl 2023. *Nucleic Acids Res.* **51**, D933–D941 (2023).
48. Soneson, C., Love, M. I. & Robinson, M. D. Differential analyses for RNA-seq: transcript-level estimates improve gene-level inferences [version 1; peer review: 2 approved]. *F1000Res.* **4**, (2015).
49. Tokar, T. *et al.* mirDIP 4.1-integrative database of human microRNA target predictions. *Nucleic Acids Res.* **46**, D360–D370 (2018).
50. Huang, H.-Y. et al. miRTarBase update 2022: an informative resource for experimentally validated miRNA-target interactions. *Nucleic Acids Res.* **50**, D222–D230 (2022).
51. Skoufos, G. *et al.* TarBase-v9.0 extends experimentally supported miRNA-gene interactions to cell-types and virally encoded miRNAs. *Nucleic Acids Res.* **52**, D304–D310 (2024).
52. Kolberg, L. et al. g:Profiler-interoperable web service for functional enrichment analysis and gene identifier mapping (2023 update). *Nucleic Acids Res.* **51**, W207–W212 (2023).
53. Merico, D., Isserlin, R., Stueker, O., Emili, A. & Bader, G. D. Enrichment map: a network-based method for gene-set enrichment visualization and interpretation. *PLoS ONE* **5**, e13984 (2010).
54. Paugh, B. S. et al. Integrated molecular genetic profiling of pediatric high-grade gliomas reveals key differences with the adult disease. *J. Clin. Oncol.* **28**, 3061–3068 (2010).
55. Suri, V. et al. Pediatric glioblastomas: A histopathological and molecular genetic study. *Neuro Oncol.* **11**, 274–280 (2009).
56. Giamanco, K. A. & Matthews, R. T. The role of behab/brevican in the tumor microenvironment: mediating glioma cell invasion and motility. *Adv. Exp. Med. Biol.* **1272**, 117–132 (2020).
57. Schaberg, E., Götz, M. & Faissner, A. The extracellular matrix molecule tenascin-C modulates cell cycle progression and motility of adult neural stem/progenitor cells from the subependymal zone. *Cell. Mol. Life Sci.* **79**, 244 (2022).
58. Hong, Q., Li, R., Zhang, Y. & Gu, K. Fibrillin 2 gene knockdown inhibits invasion and migration of lung cancer cells. *Cell Mol. Biol. (Noisy-le-grand)* **66**, 190–196 (2020).
59. Dewdney, B. et al. From signalling pathways to targeted therapies: Unravelling glioblastoma's secrets and harnessing two decades of progress. *Signal Transduct. Target. Ther.* **8**, 400 (2023).
60. Sakakini, N. et al. A positive feed-forward loop associating EGR1 and PDGFA promotes proliferation and self-renewal in glioblastoma stem cells. *J. Biol. Chem.* **291**, 10684–10699 (2016).
61. Shin, C. H. et al. HBEGF promotes gliomagenesis in the context of Ink4a/Arf and Pten loss. *Oncogene* **36**, 4610–4618 (2017).
62. Pang, Y., Zhou, S., Zumbo, P., Betel, D. & Cisse, B. TCF12 deficiency impairs the proliferation of glioblastoma tumor cells and improves survival. *Cancers (Basel)* **15**, (2023).
63. Liu, Z.-G. et al. c-Fos over-expression promotes radioresistance and predicts poor prognosis in malignant glioma. *Oncotarget* **7**, 65946–65956 (2016).
64. Zhou, S. et al. The MAP3K1/c-JUN signaling axis regulates glioblastoma stem cell invasion and tumor progression. *Biochem. Biophys. Res. Commun.* **612**, 188–195 (2022).
65. Pascual-García, M. et al. LIF regulates CXCL9 in tumor-associated macrophages and prevents CD8+ T cell tumor-infiltration impairing anti-PD1 therapy. *Nat. Commun.* **10**, 2416 (2019).
66. Tatari, N. et al. The proteomic landscape of glioblastoma recurrence reveals novel and targetable immunoregulatory drivers. *Acta Neuropathol.* **144**, 1127–1142 (2022).
67. Novak, M. *et al.* CCR5-mediated signaling is involved in invasion of glioblastoma cells in its microenvironment. *Int. J. Mol. Sci.* **21**, (2020).
68. Dai, L. et al. Identification and validation of SOCS1/2/3/4 as potential prognostic biomarkers and correlate with immune infiltration in glioblastoma. *J. Cell. Mol. Med.* **27**, 2194–2214 (2023).
69. Guessous, F. et al. Oncogenic effects of miR-10b in glioblastoma stem cells. *J. Neurooncol.* **112**, 153–163 (2013).
70. Li, S.-Z. et al. miR-139/PDE2A-Notch1 feedback circuit represses stemness of gliomas by inhibiting Wnt/β-catenin signaling. *Int. J. Biol. Sci.* **17**, 3508–3521 (2021).
71. Cai, S. *et al.* miR-124-3p inhibits the viability and motility of glioblastoma multiforme by targeting RhoG. *Int. J. Mol. Med.* **47**, (2021).
72. Ruoslahti, E. Brain extracellular matrix. *Glycobiology* **6**, 489–492 (1996).
73. Wiranowska, M. & Rojiani, M. V. Extracellular matrix microenvironment in glioma progression. In *Glioma—Exploring Its Biology and Practical Relevance* (ed. Ghosh, A.) (InTech, 2011). https://doi.org/10.5772/24666.
74. Ulrich, T. A., de Juan Pardo, E. M. & Kumar, S. The mechanical rigidity of the extracellular matrix regulates the structure, motility, and proliferation of glioma cells. *Cancer Res.* **69**, 4167–4174 (2009).
75. Umesh, V., Rape, A. D., Ulrich, T. A. & Kumar, S. Microenvironmental stiffness enhances glioma cell proliferation by stimulating epidermal growth factor receptor signaling. *PLoS ONE* **9**, e101771 (2014).
76. Forsyth, P. A. et al. Gelatinase-A (MMP-2), gelatinase-B (MMP-9) and membrane type matrix metalloproteinase-1 (MT1-MMP) are involved in different aspects of the pathophysiology of malignant gliomas. *Br. J. Cancer* **79**, 1828–1835 (1999).
77. Nakada, M. et al. Suppression of membrane-type 1 matrix metalloproteinase (MMP)-mediated MMP-2 activation and tumor invasion by testican 3 and its splicing variant gene product. *N-Tes. Cancer Res.* **61**, 8896–8902 (2001).
78. Bouterfa, H. et al. Expression of different extracellular matrix components in human brain tumor and melanoma cells in respect to variant culture conditions. *J. Neurooncol.* **44**, 23–33 (1999).
79. Mahesparan, R. et al. Expression of extracellular matrix components in a highly infiltrative in vivo glioma model. *Acta Neuropathol.* **105**, 49–57 (2003).
80. Grabowska, M. et al. miR-218 affects the ECM composition and cell biomechanical properties of glioblastoma cells. *J. Cell. Mol. Med.* **26**, 3913–3930 (2022).
81. Wang, Y. et al. COL1A2 inhibition suppresses glioblastoma cell proliferation and invasion. *J. Neurosurg.* **138**, 639–648 (2023).
82. Bai, J. et al. HIF-1α-mediated LAMC1 overexpression is an unfavorable predictor of prognosis for glioma patients: evidence from pan-cancer analysis and validation experiments. *J. Transl. Med.* **22**, 391 (2024).

83. Ramírez, E. et al. Glioblastoma invasiveness and collagen secretion are enhanced by vitamin C. *Antioxid. Redox Signal.* **37**, 538–559 (2022).
84. Tsai, H.-F. et al. Type V collagen alpha 1 chain promotes the malignancy of glioblastoma through PPRC1-ESM1 axis activation and extracellular matrix remodeling. *Cell Death Discov.* **7**, 313 (2021).
85. Kaufman, L. J. et al. Glioma expansion in collagen I matrices: analyzing collagen concentration-dependent growth and motility patterns. *Biophys. J.* **89**, 635–650 (2005).
86. Fang, M., Yuan, J., Peng, C. & Li, Y. Collagen as a double-edged sword in tumor progression. *Tumour Biol.* **35**, 2871–2882 (2014).
87. Kefas, B. et al. microRNA-7 inhibits the epidermal growth factor receptor and the Akt pathway and is down-regulated in glioblastoma. *Cancer Res.* **68**, 3566–3572 (2008).
88. Mathew, L. K. *et al.* Feedback circuitry between miR-218 repression and RTK activation in glioblastoma. *Sci. Signal.* **8**, ra42 (2015).
89. Gu, J. et al. miR-218-5p inhibits the malignant progression of glioma via targeting TCF12. *Tumori* **108**, 338–346 (2022).
90. Chatterjee, B. *et al.* MicroRNAs: As critical regulators of tumor- associated macrophages. *Int. J. Mol. Sci.* **21** (2020).
91. Zhao, G. et al. M2-like tumor-associated macrophages transmit exosomal miR-27b-3p and maintain glioblastoma stem-like cell properties. *Cell Death Discov.* **8**, 350 (2022).
92. Zhou, R. et al. Evidence for selective microRNAs and their effectors as common long-term targets for the actions of mood stabilizers. *Neuropsychopharmacology* **34**, 1395–1405 (2009).
93. Taylor, K. R. et al. Glioma synapses recruit mechanisms of adaptive plasticity. *Nature* **623**, 366–374 (2023).
94. Venkatesh, H. S. et al. Electrical and synaptic integration of glioma into neural circuits. *Nature* **573**, 539–545 (2019).
95. Venkataramani, V. et al. Glutamatergic synaptic input to glioma cells drives brain tumour progression. *Nature* **573**, 532–538 (2019).
96. Mullard, A. FDA approves fifth RNAi drug—Alnylam's next-gen hATTR treatment. *Nat. Rev. Drug Discov.* **21**, 548–549 (2022).

Acknowledgements

Author contributions

I.A.G., A.R. and L.S. conceptualized and interpreted the results. I.A.G. and A.R. conducted data curation and analysis. J.T.S.C. and T.J.S. also contributed to data analysis. I.A.G., A.R. and L.S. wrote the paper. All authors revised and approved the manuscript.

Declarations

Competing interests

The authors declare no competing interests.

Additional information

Supplementary Information The online version contains supplementary material available at https://doi.org/10.1038/s41598-024-78337-y.

Correspondence and requests for materials should be addressed to L.S.

Reprints and permissions information is available at www.nature.com/reprints.

Publisher's note Springer Nature remains neutral with regard to jurisdictional claims in published maps and institutional affiliations.